



ORIGINAL ARTICLE

Synthesis of yttrium doped nanocrystalline ZnO and its photocatalytic activity in methylene blue degradation



P.K. Sanoop^a, S. Anas^a, S. Ananthakumar^a, V. Gunasekar^b, R. Saravanan^b, V. Ponnusami^{b,*}

^a Materials and Minerals Division, National Institute for Interdisciplinary Science and Technology (CSIR), Thiruvananthapuram 695 019, Kerala, India

^b School of Chemical and Biotechnology, SASTRA University, Thirumalaisamudram, Thanjavur 613 401, Tamilnadu, India

Received 21 September 2011; accepted 23 April 2012
Available online 1 May 2012

KEYWORDS

Microwave irradiation;
ZnO;
Yttria doping;
Photocatalytic oxidation;
Methylene blue

Abstract Yttrium doped zinc oxide was prepared by microwave irradiation of $Y(NO_3)_3 \cdot 6H_2O$ and $Zn(NO_3)_2 \cdot 4H_2O$ as precursors, in ethanol–water medium. Highly polar ethanol–water medium (30/70, v/v) with hexamine and urea assist the formation of ZnO nuclei very rapidly in a specific fashion. Furthermore, Y^{3+} ions infiltration into $Zn(OH)_2$ precipitate was facilitated by microwaves (2.45 GHz, 950 W). Yttrium doped nanocrystalline ZnO (ZnO-99 and ZnO-95) was formed with 1 and 5 mol% yttrium precursor. The powder was morphologically characterized with XRD, DLS, SEM and TEM. Photocatalytic activity of microwave treated Y^{3+} doped ZnO was tested by studying the oxidation of methylene blue solution in a batch reactor. The studies showed that the catalytic reaction followed second order kinetics. Based on the results obtained from photocatalytic studies, efficiencies of various ZnO samples were found to be in this order: ZnO-A > ZnO-99 > ZnO-95 > ZnO-R that is, Y^{3+} doped ZnO was not as effective as commercial undoped ZnO. However, ZnO-95 had shown better stability, antiphotocorrosive nature and reusability among the samples tested in this study.

© 2012 Production and hosting by Elsevier B.V. on behalf of King Saud University. This is an open access article under the CC BY-NC-ND license (<http://creativecommons.org/licenses/by-nc-nd/3.0/>).

1. Introduction

Textile industry is water-intensive and hence generates a large amount of harmful dye effluent (Akyol et al., 2004). With more and more increasing awareness on environment stringent norms are being specified by the government in many countries (Gupta and Suhas, 2009). However, owing to the dyes' complex chemical/molecular structures and inherent toxicity, removal of dyes completely from the effluent became difficult

* Corresponding author. Tel.: +91 4362 264101; fax: +91 4362 264120.

E-mail address: vponnu@chem.sastra.edu (V. Ponnusami).
Peer review under responsibility of King Saud University.



Production and hosting by Elsevier

Nomenclature

r	photocatalytic reaction rate ($\text{mg}/\text{dm}^3 \text{ s}$)	k_{2a}	second order reaction rate constant ($[\text{mg}/\text{dm}^3]^{-1} \text{ s}^{-1}$)
C_{MB}	concentration of MB in solution (mg/dm^3)	K_{ad}	adsorption coefficient
t	time (s)	$K_{\text{L-H}}$	Langmuir–Hinshelwood reaction rate constant (s^{-1})
k_{1a}	apparent first order reaction rate constant (s^{-1})		

by conventional physico-chemical treatments like adsorption, coagulation and ion-exchange (Ponnusami and Srivastava, 2009; Kashefialasl et al., 2006; Wu et al., 2008a,b). Moreover, these treatments only transfer contaminants from one phase to another and fail to completely demineralize the toxic pollutants (Daneshvar et al., 2004).

Advanced oxidation processes have gained better acceptance in the recent past because they have capability to effectively mineralize the pollutants (Li et al., 2008; Wu et al., 2008a,b). TiO_2 , TiO_2 -membranes, and TiO_2 nanotubes are widely used as photocatalysts (Daneshvar et al., 2004; Li et al., 2008; Barka et al., 2010). Literature reports indicate that the nano-ZnO material can also function as an efficient photocatalyst in the presence of UV light (Jiang et al., 2008). Irradiation of the semi conducting ZnO with UV light results in the formation of an electron–hole pair due to photo-excitation. The hole thus formed possesses high oxidation potential that can directly oxidize the organic pollutants (Morrison and Freund, 1967; Sancier and Morrison 1973). Also, the UV irradiation can produce highly reactive hydroxyl radicals, by splitting water, which in turn breaks up the organic molecules leading to complete mineralization. Electron in the conduction band may also produce highly reactive peroxide radicals that can take part in the mineralization reaction (Daneshvar et al., 2004).

ZnO is a hexagonal, wurtzite type semi conducting oxide with the energy band gap close to TiO_2 . For the effective degradation of the dye molecules, the catalyst might have increased surface area as well as catalytically active surface sites. It calls for tuning the catalyst surface morphology either by suitable surfactant assisted chemical coupling techniques or the growth of nanostructures over crystallographically oriented substrates. In this respect, ZnO is advantageous because of its characteristic features such as (i) wide scope for easy tuning of the surface morphologies into a varieties of nanostructures (Moghaddam et al., 2009), (ii) simple processing at low temperatures for forming nanocrystalline ZnO (Perales-Perez et al., 2004), (iii) large concentrations of lattice defects and oxygen vacancies in the crystal structures (Kohan et al., 2000), (iv) low temperature regenerative capacity (Hassan, 2010) and (v) low price (Amornpitoksuk et al., 2011). These features make the material ideal for industrial photocatalysis applications. Due to the excellent photo reactivity, non toxicity, and long-term stability, commercial interest is high to make photoactive nano-ZnO. Processing techniques ranging from simple reflux to hydrothermal or sonochemical reactions with or without surfactants and templates are reported for obtaining high surface area nano-ZnO photocatalysts (Li and Haneda, 2003; Andelman et al., 2005; Sun et al., 2004). We have earlier reported the preparation of photocatalytic nano-ZnO via microwave assisted citrate gel decomposition.

Microwaves interact with zinc metal complexes and gels so rapidly that it converts the matter into fully crystalline nanoceramic particles within a few minutes. Development of micro/macro porosities with enhanced pore volume is also very much possible by microwave techniques (Hammad et al., 2009; Jung et al., 2006). Apart from these, microwave heating is able to produce unusual particle morphologies and porous nanoclusters. ZnO doped with Ag^{2+} and Al^{3+} was also prepared and the structural and functional properties were assessed (Ananthakumar et al., 2010). The major benefits of yttrium doping are (i) Yttrium doping decrease energy band gap of ZnO (Hammad et al., 2009), (ii) the Y^{3+} surface enrichment hinders crystallite growth (Atriabak et al., 2009) and (iii) the surface segregation of Y^{3+} promotes oxygen vacancies creation (Atriabak et al., 2009). Yttria doping is likely to increase the photo catalytic efficiency of ZnO due to above mentioned reasons. On this basis we have chosen yttrium as dopant. In the present work microwave irradiated yttria doped ZnO has been prepared and UV-photocatalytic property has been compared with the commercially available nano-ZnO.

2. Experimental

2.1. Materials and methods

Analytical grade zinc nitrate tetrahydrate (Central Drug House (Pvt.) Ltd., 99%), yttrium nitrate (CDH, Mumbai, 99.9%), hexamine and urea (S.D. Fine-Chemicals Ltd., 99%) were used as reactants and all the reagents were used in the as-received condition. 20% diluted HNO_3 solution was used for controlling the pH. Double distilled water and ethanol were used as the media. Commercial ZnO (99.9%) was procured from Aldrich Chemicals Company Inc., USA.

Analytical grade Methylene blue (MB, Chemical formula: $\text{C}_{16}\text{H}_{18}\text{N}_3\text{SCl}$; FW: $319.86 \text{ g mol}^{-1}$, $\lambda_{\text{max}} = 662 \text{ nm}$, class: thiazine, C.I. Classification Number: 52015.) supplied by Himedia India Limited was used in the photo-catalysis study. The dye was used in as received condition. Dye solution was prepared by dissolving the required amount of dye in double distilled water. Concentration of MB in the aqueous solution was determined by measuring the light absorbance (OD) at its characteristic wavelength 662 nm using UV–vis. Spectrophotometer (Elico – SL 150). Samples were diluted wherever necessary to maintain the OD below 1.0.

2.1.1. Synthesis of ZnO photocatalysts

In a typical experiment, Zn (NO_3) $_2$ ·4 H_2O , hexamine, and urea reactants were taken in the molar ratios of 0.5:1:1 and dissolved in ethanol + water (30/70, v/v ratio) mixture. The initial pH of the precursor solution was controlled at pH 3.0 by

adding a few drops of dilute HNO_3 . Yttrium nitrate solution having 0.05 M concentration was separately prepared for the doping. First, the zinc precursor solution containing hexamine and urea was mechanically stirred for 2 h and then kept in a conventional microwave oven (Electrolux, 950 W, 2.45 GHz). The microwave input power level of 300 W was employed during this gelling step. The solution turned into a viscous liquid in 10 min yielding thick gelatinous hydrated zinc oxy hydroxide white precipitate. It was further treated with yttrium nitrate doping solution equivalent to the doping levels of 1 and 5 mol%. The hydrated $\text{Zn}(\text{OH})_2$ precipitate turns into colloidal suspension when it is re-dispersed ultrasonically into yttrium nitrate solution. The milky colloid was again subjected to microwaves at 500 W for nearly an hour. Finally thick white gel flakes were obtained. Flakes were collected and transferred into an alumina crucible (120 ml capacity) and again subjected to microwaves at a power of 950 W. The precursor gel flakes got heated up rapidly. As the exposure time continued the reaction mixture started to decompose releasing brown nitrogen oxides fumes. Within a short exposure time of 15 min a porous white residue was obtained. At this stage the reaction was stopped. The rise in reactant temperature was not measured but once the reaction was stopped the temperature inside the alumina crucible was measured and found to be 360°C . The powder was collected after cooling and ground simply by a mortar-pestle. After grinding, it was transferred again into an alumina crucible and subjected to microwave assisted calcination. The calcination was carried out at 950 W for 30 min. The temperature inside the crucible was measured using an external thermocouple and it was observed as $485 \pm 20^\circ\text{C}$. The microwave calcination finally resulted in a light yellow ZnO powder. In these experiments two sets of Yttrium doped ZnO samples were produced. The sample details are presented in Table 1. Undoped ZnO sample (ZnO-R) was prepared in the same manner as described above, but without yttrium doping.

2.1.2. Characterizations of ZnO catalyst

The crystalline nature and phase evolution of the microwave irradiated and calcined ZnO samples were analyzed by powder X-ray diffraction using a Philips, X'pert Pro with a monochromator on the diffraction beam side (Cu $K\alpha$ radiation, $\lambda = 0.154$ nm). The crystallite size of the powder was calculated using Scherrer's equation. The ZnO powder morphology was probed using transmission electron microscopy (TEM). TEM images were captured using JEOL JEM 2000X, using carbon coated copper grids. Selected area electron diffraction (SAED) patterns using TEM were also taken to identify the crystalline nature of the samples.

Table 1 Preparation of microwave treated yttria doped ZnO samples.

S. No	Experimental conditions	Sample notation
1.	Zinc nitrate + HMTA + Urea + Ethanol (pH~3)	ZnO-R
2.	$\text{Zn}(\text{OH})_2$ + 5 mol% Y_2O_3	ZnO-95
3.	$\text{Zn}(\text{OH})_2$ + 1 mol% Y_2O_3	ZnO-99
4.	Aldrich ZnO	ZnO-A

2.1.3. Photochemical reactor

The photochemical reactor assembly (Model IWQ1) supplied by SAIC India Ltd., Chennai, was used for the photochemical studies. A medium pressure mercury lamp (125 W) was used as light source. The lamp was housed in an immersion well which was provided with a cooling water jacket. Air, the oxygen source, was supplied using a small aquarium blower unit. The samples were withdrawn from the bottom of the reactor periodically. The Teflon filter provided at the bottom of the reactor was useful to minimize the carry-over of solid catalysts along with the samples.

2.2. Degradation kinetics

Pseudo first order, pseudo second order and Langmuir-Hinshelwood kinetic expressions were widely used by majority of the researchers today to describe the photocatalytic oxidation of organics compounds (Baran et al., 2008; Hermann, 1999; Wu et al., 2006; Kim et al., 2008; Behnajady et al., 2006; Al-Ekabi and Serpone, 1988; Beltran-Heredia et al., 2001). Pseudo first order kinetics is a special form of L-H kinetics (Baran et al., 2008; Kim et al., 2008). These models are expressed by the following expressions:

$$\ln \frac{C_0}{C_{MB}} = k_{1a}t \quad (1)$$

$$\frac{1}{C_{MB}} = \frac{1}{C_o} + k_2t \quad (2)$$

$$r_{L-H} = -\frac{dC_{MB}}{dt} = \frac{K_{ad}kC_{MB}}{1 + K_{ad}C_o} = K_{L-H}C_{MB} \quad (3)$$

3. Results and discussion

3.1. Characterization of microwave derived ZnO

Microwave irradiation of the solution of the precursors $\text{Zn}(\text{NO}_3)_2 \cdot 4\text{H}_2\text{O}$, $(\text{CH}_2)_6\text{N}_4$ and $\text{NH}_2\text{CO} \cdot \text{NH}_2$ underwent

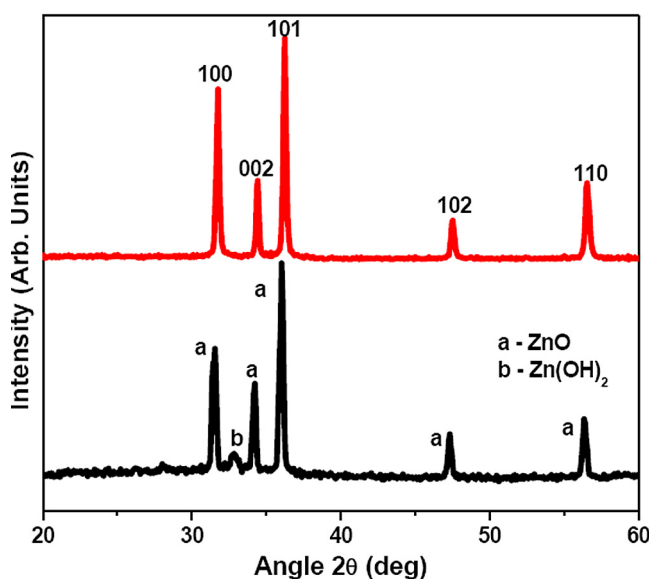


Figure 1 X-ray analysis of microwave irradiated ZnO samples [Bottom curve: 2 min irradiation, Top curve: 10 min irradiation].

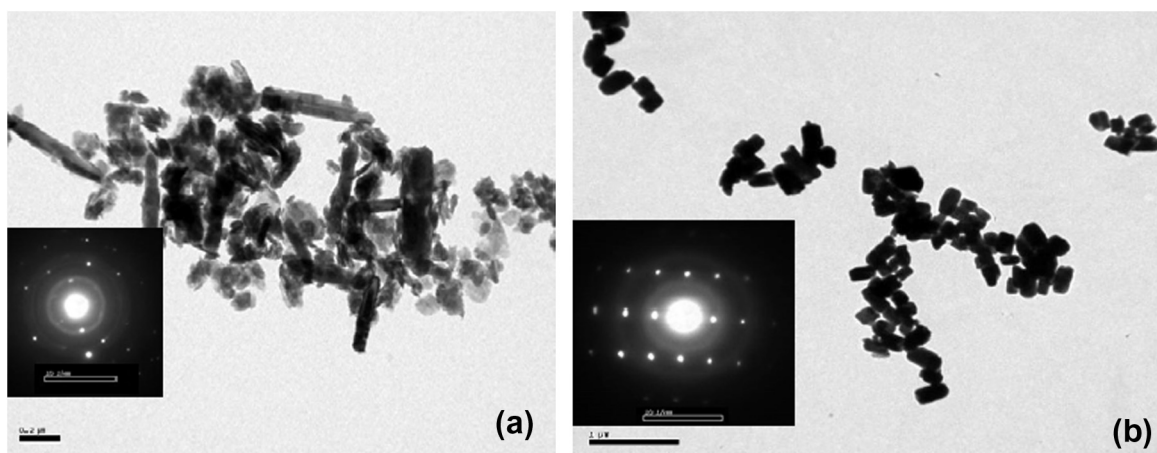


Figure 2 TEM images of ZnO particles (a) particle evolution at 2 min irradiation to microwaves (pH 7.2) (b) 10 min (pH 8.7).

hydrolysis due to ammonia release forming hydrated $\text{Zn}(\text{OH})_2$. The hydrolysis reaction started to occur within 2 min of irradiation which was monitored by measuring the change in pH value of the reactant solution. The solution mixture exposed for 2 min yielded a pH value of 7.2. In fact at pH below 8, the zinc precursor solution was expected to undergo only partial hydrolysis and therefore the irradiation time was increased till the pH changed between 8 and 10. However, the rapid heat generation within the reaction mixture and continuous drying of the solvent resulted in a viscous gel within 10 min. The gel after cooling had the pH of 8.2. The powder X-ray diffraction patterns of the ZnO samples at different time intervals are presented in Fig. 1. The samples irradiated for 10 min at the microwave power of 500 W shows a mixture of crystalline ZnO and $\text{Zn}(\text{OH})_2$ phases confirming the partial hydrolysis of the system. Once the irradiation time increased at increased microwave power, fully crystalline ZnO phases were obtained.

All diffraction peaks are similar to those of a bulk wurtzite ZnO, which has a hexagonal structure [lattice parameter $a = 3.22 \text{ \AA}$, $c = 5.2 \text{ \AA}$, space group P63mc], and their diffraction data are in good agreement with the JCPDS file (75–1526).

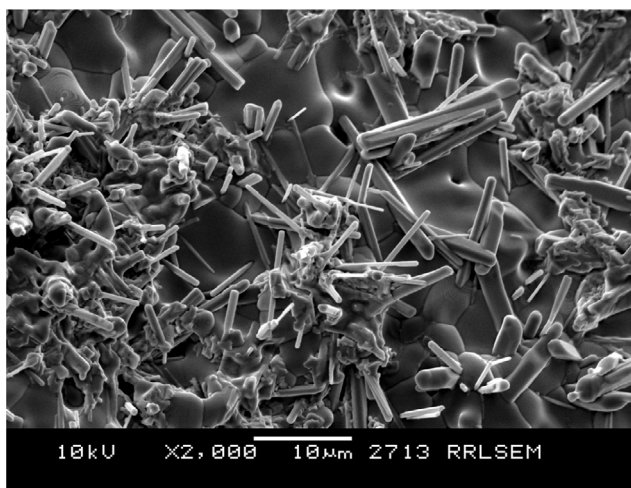


Figure 3 SEM image of ZnO 95% sample microwave irradiated for 1 h at 950 W.

The primary crystallite size $D = 36 \text{ nm}$ was determined from the (101) peak. Microwave heating was a net effect of molecular scale interactions of the matter with microwave energy that largely depend upon the polarization efficiency of the system. Microwave assisted hydrolysis involving urea and hexamine was earlier reported mainly for the reasons that these substances readily absorbed microwaves and the rate of nuclei formation was so instant due to faster reaction kinetics. In this case the water and ethanol mixture was also highly polar that could assemble the ZnO nuclei in a specific fashion. Fig. 2 shows the TEM images of the ZnO crystals formed by microwave assisted nucleation and growth.

Fig. 2a shows the particle morphologies of the ZnO samples formed after 2 min of microwave irradiation where the partial hydrolysis occurred. At this stage the images indicate that the crystallization was not complete and that the powders had fine-clusters and partly grown rods and needles. However, when the samples were carefully exposed for longer time (10 min) under microwaves, the particles had grown completely into well-ordered hexagonal crystals (Fig. 2b). TEM images show the particle sizes of the ZnO samples in the range of 200–250 nm. It was compared with the particle size distribution data obtained by DLS measurements. The segregation of excess yttria can be confirmed from the SEM image in Fig. 3 taken on the ZnO powder lump irradiated to microwaves for 1 h at 950 W. The image clearly shows the growth of dense crystalline, hexagonal ZnO rods over liquid phase yttria matrix. However, the average width of the hexagonal crystals is marginally enhanced compared to the undoped ZnO counterparts. Fig. 4 presents the DLS analysis of the ZnO samples after irradiation at 500 and 950 W microwave powers. These powders after milling in the presence of polyacrylate dispersant for 2 h and ultrasonication shows the average particle size as 185 and 225 nm respectively. These particles were further used for the decolourization of methylene blue dyes in UV light.

3.2. Dye degradation studies

3.2.1. Comparison of ZnO catalysts

In order to examine the UV-catalytic efficiency of the ZnO samples, 150 ml of 80 ppm MB solution was first taken in a beaker and 10 mg of ZnO based catalyst was added to it.

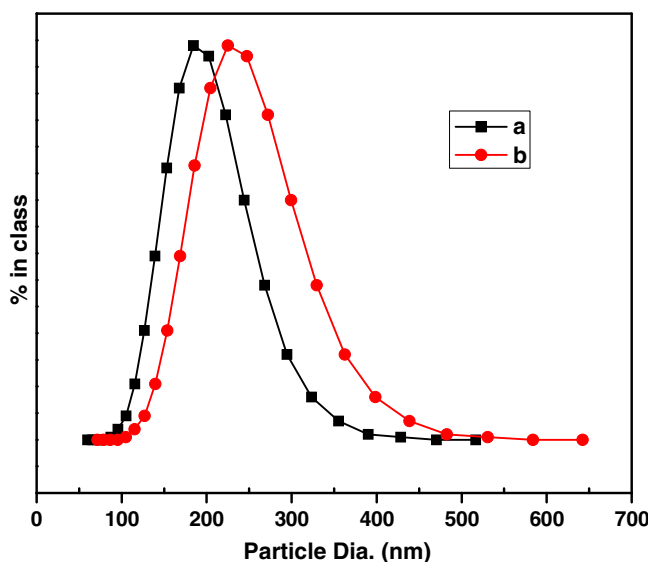


Figure 4 Particle size distribution analysis of ZnO-99% sample microwave irradiated for 30 min at (a) 500 W (b) 950 W.

Photocatalytic degradation was carried out using ZnO-A (commercial undoped), ZnO-95 (doped with 5 mol% yttria), ZnO-99 (doped with 1 mol% yttria) and ZnO-R (undoped ZnO prepared by irradiation). The mixture was then transferred to the UV-reactor and air was supplied continuously as shown in Fig. 5. For the first fifteen minutes UV irradiation was not given. After that UV irradiation was started. However, samples were collected at zero and fifteen minutes for comparison. During reaction, samples were taken at regular intervals, and then centrifuged. The supernatant was analyzed for MB concentration.

Concentration decay curves of methylene blue solutions are shown in Fig. 6. Prior to UV light irradiation there was a drop in the MB concentration due to adsorption of MB onto the catalysts powders which was not appreciable, however, immediately after UV irradiation, concentration of MB decreased rapidly. This confirmed that all the catalysts used in this study oxidized MB dye effectively in the presence of UV light. It is

evident from the figure that photo-catalytic efficiencies of ZnO-95 and ZnO-99, as measured by the disappearance of MB, were nearly equal to that of commercial ZnO. 90% of MB was reduced in 100, 60, 60, 40 min by ZnO-R, ZnO-99, ZnO-95, and ZnO-A respectively. Thus, the photocatalytic efficiency of the various ZnO catalysts used in this study can be put in this order: ZnO-A > ZnO-99 > ZnO-95 > ZnO-R. It could also be noticed that initial adsorption of MB by these ZnO catalysts prior to UV irradiation was in the same order. That is an increase in adsorption efficiency of the catalysts used resulted in corresponding increase in photodegradation rate. This observation is consistent with the heterogeneous catalysis theory (Baran et al., 2008; Mangalampalli et al., 2008). However, it is understood that doping of yttria slightly affects the dye adsorption capacity of the ZnO samples that significantly decrease the photocatalytic activity. Earlier reports on sol gel derived yttria doped ZnO coatings indicate that yttria in ZnO lattice acquires substitutional position at low concentration while at higher concentrations, it takes the interstitial sites. Moreover, the addition is very effective only if 5% Yt is doped (Ravinder et al., 2006). The adsorption capacity of ZnO-R was very much lower than that of commercial ZnO and Y^{3+} doped ZnO. In the case of undoped counterpart the microwave irradiation might have resulted in sintering of the individual nanocrystallites within the clusters possibly destroying the active sites on the catalysts. Yttria is a recognized high temperature rare earth oxide and doping has favored the thermal stability of ZnO and ultimately resulted in comparable performance.

3.2.2. Degradation kinetics

Effect of initial dye concentration was studied by conducting a series of experiments with different initial dye concentrations (e.g. 40, 60, 80 or 100 mg/dm³) with constant catalyst loading. Best fitting kinetic model was chosen using linear regression method. It was observed that photodegradation of MB by ZnO-R, ZnO-99 and ZnO-A followed first order kinetics with high R^2 values. On the other hand, MB degradation by ZnO-95 followed second order kinetics. Figs. 7 and 8 depict the kinetics of MB degradation under UV catalytic activities by the ZnO-R, ZnO-99, ZnO-95, and ZnO-A photocatalysts.

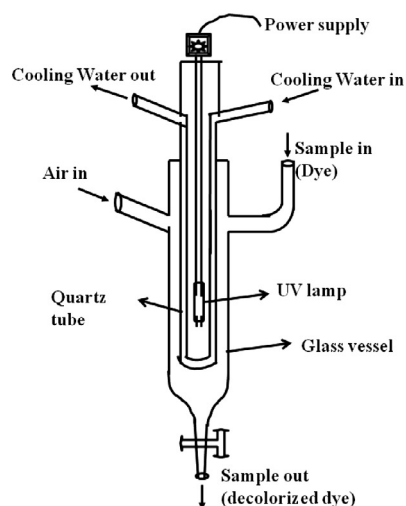


Figure 5 Schematic and photographic images of photocatalytic reactor (reactor in OFF condition for visibility of reactor parts).

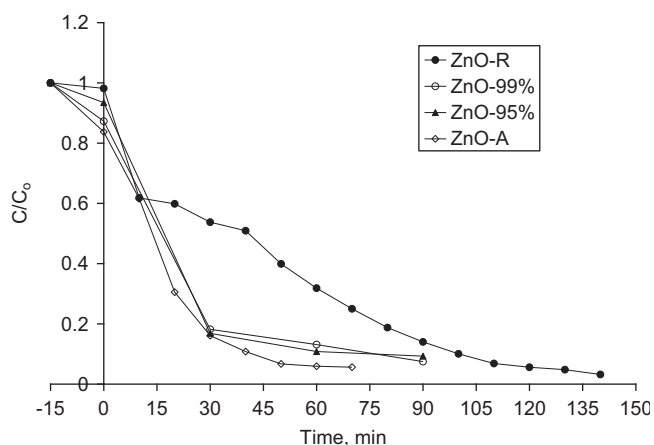


Figure 6 Concentration decay curve of MB solution before and after UV irradiation [volume of solution = 150 cm³; catalysts used ZnO-R, ZnO-95%, ZnO-99% and ZnO-A; Initial dye concentration = 80 mg/dm³, amount of catalysts used = 66.67 mg/dm³].

Table 2 gives the comparative kinetic parameters and the corresponding coefficients of determination for the MB photodegradation reaction by ZnO. It is observed that ZnO-R, ZnO-99 and ZnO-A degraded MB according to first order kinetics. In fact most of the previous studies have strongly reported first order photodegradation kinetics of MB organic dyes under UV. The present findings also have good agreement with the reported works for all the samples except the one having 5 mol% yttria additions [ZnO-95]. In this case the degradation reaction follows second order kinetics. The microwave

irradiation and its heating effect strongly vary with respect to the dielectric nature of the constituent materials. ZnO is a known semi conducting ceramic with dielectric constant ranging from 8.9–10.2. Whereas Y₂O₃ has a dielectric constant close to 20 which is two orders more than ZnO. Therefore the microwave induced dielectric heating is very rapid that preferably allows the segregation of excess yttrium ions outside ZnO structure producing ZnO + Y₂O₃ composite phases. Since the energy band gap of yttria is around 5.8 eV, which is again two orders high compared to ZnO, the net UV absorption by the composite phase decreased effectively that reflects as second order kinetics in the ZnO samples having high amounts of Y₂O₃ doping.

3.2.3. Effect of pH

Effect of pH on photocatalytic efficiency of the samples was investigated at pH 4, 7 and 10. The results are shown in Fig. 9. The photocatalytic efficiencies of ZnO samples increased with increase in pH. Highest percentage color removal was achieved at pH 10 for all these samples.

3.2.4. Reusability studies

150 ml of 80 ppm MB solution was taken in the photoreactor and 66.67 mg/dm³ ZnO sample (ZnO-A/ZnO-R/ZnO-99/ZnO-95) was added to that. The sample was subjected to UV irradiation for 150 min. At the end of 150 min the reaction was stopped, and the solution was centrifuged to separate the catalyst from the solution. The supernatant solution was analyzed for MB composition as described above in Section 2.1 and the recovered catalyst was reused in the next run. This procedure was repeated for 4 runs. Results are shown in the Fig. 10. Reusability of the catalysts were found to be in this

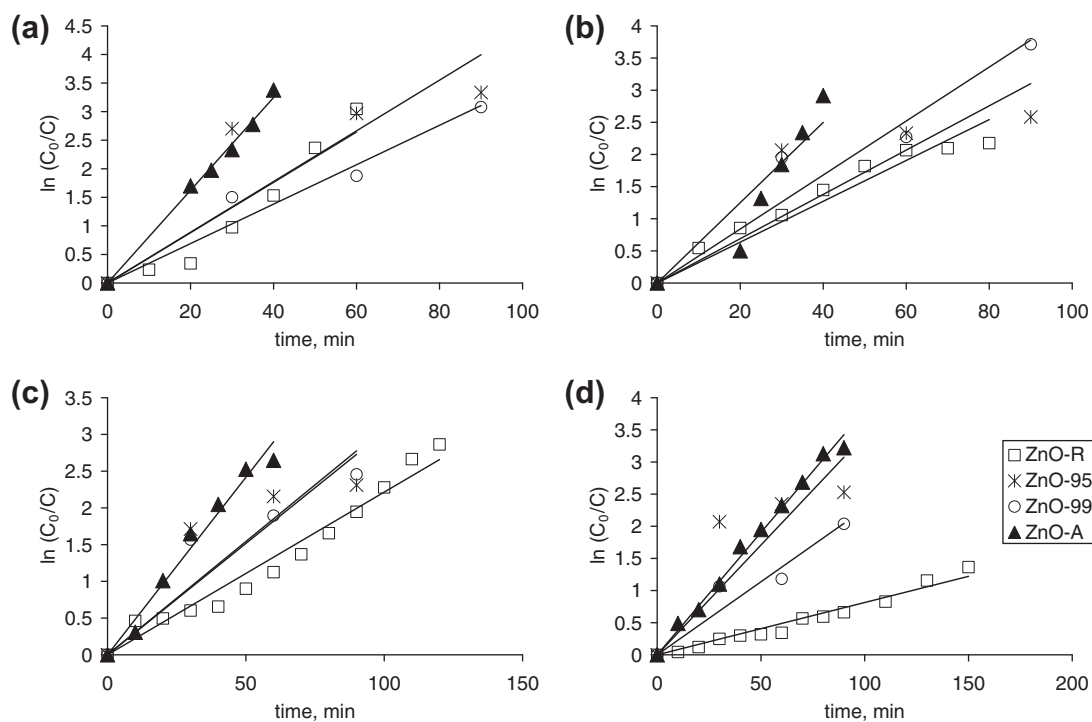


Figure 7 Methylene blue photooxidation by ZnO based photo catalysts – first order reaction kinetics. ((a) C₀ = 40 ppm; (b) C₀ = 60 ppm; (c) C₀ = 80 ppm; (d) C₀ = 100 ppm).

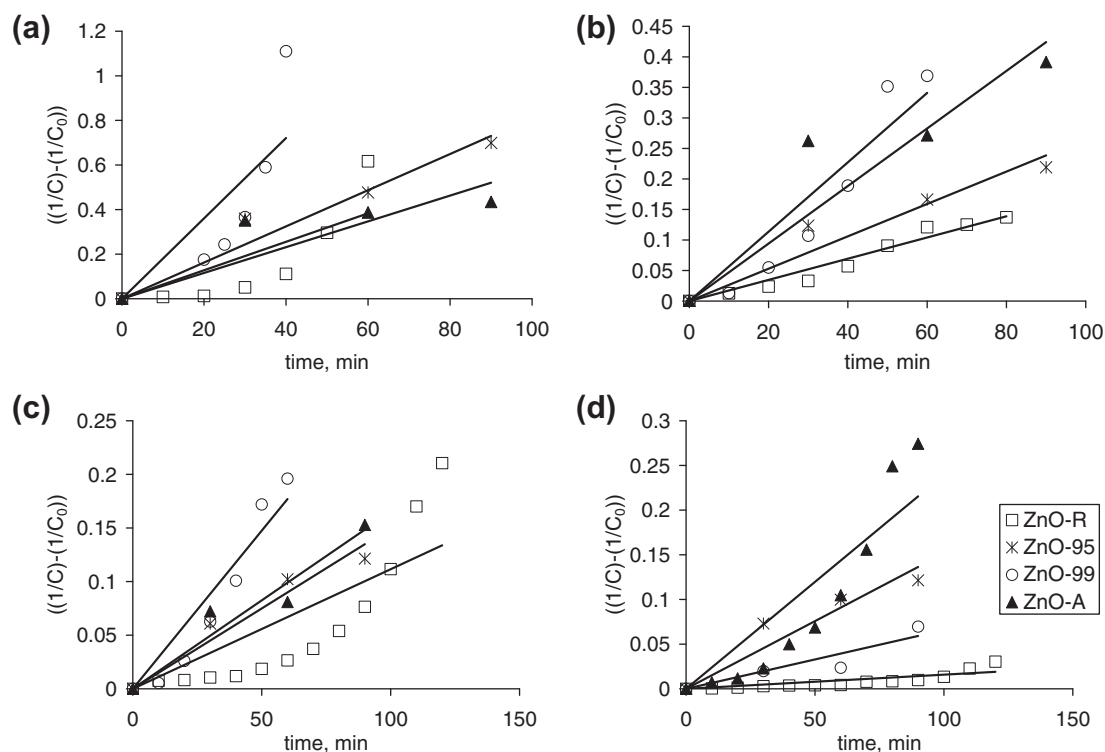


Figure 8 Methylene blue photooxidation by ZnO based photo catalysts – second order reaction kinetics. ((a) $C_0 = 40$ ppm; (b) $C_0 = 60$ ppm; (c) $C_0 = 80$ ppm; (d) $C_0 = 100$ ppm).

Table 2 Kinetics for MB photo-degradation by various ZnO catalysts.

	Concentration, ppm	First order		Second order	
		K_1	R^2	K_2	R^2
ZnO-R	40	0.0440	0.9135	0.0064	0.6407
	60	0.0318	0.9227	0.0017	0.9561
	80	0.0223	0.9735	0.0011	0.7002
	100	0.0082	0.9779	0.0002	0.7268
ZnO-95	40	0.0444	0.6544	0.0081	0.9437
	60	0.0345	0.6649	0.0027	0.9094
	80	0.0308	0.7241	0.0015	0.9325
	100	0.0342	0.6409	0.0015	0.8755
ZnO-99	40	0.0320	0.9558	0.0058	0.6562
	60	0.0382	0.9366	0.0047	0.8061
	80	0.0257	0.8911	0.0016	0.9266
	100	0.0208	0.9264	0.0007	0.8612
ZnO-A	40	0.0812	0.9940	0.0180	0.6633
	60	0.0554	0.9690	0.0057	0.8861
	80	0.0483	0.9756	0.0030	0.9043
	100	0.0381	0.9917	0.0024	0.8125

order ZnO-95 > ZnO-99, ZnO-A > ZnO-R. Photocatalytic efficiency of the catalysts, especially ZnO, decreases during reuse due to photo-corrosion (Fu et al., 2008; Velmurugan et al., 2011). Since the activity of ZnO-95% did not decrease significantly after four cycles it was confirmed that Yt doping improved stability and antiphotocorrosive nature of ZnO.

4. Conclusion

Dense nanocrystalline ZnO containing 1 and 5 mol% yttria was prepared by microwave irradiation and its UV-catalytic activity was studied. The technique produced hexagonal, wurtzite ZnO within 30 min of microwave irradiation with a particle size

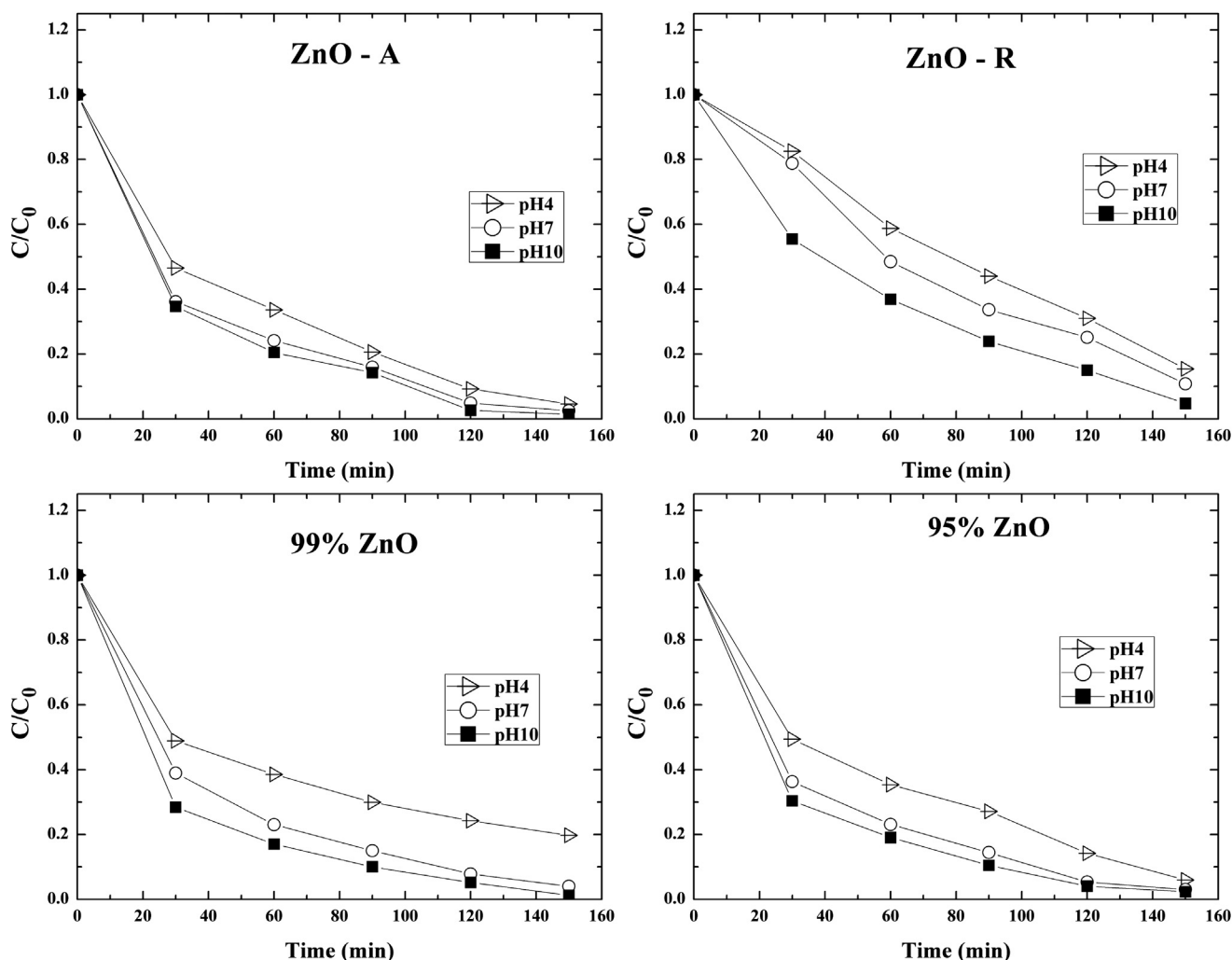


Figure 9 Methylene blue photooxidation by ZnO based photo catalysts – Effect of initial solution pH. [Volume of solution = 150 cm^3 ; catalysts used ZnO-R, ZnO-95%, ZnO-99% and ZnO-A; Initial dye concentration = 80 mg/dm^3 , amount of catalysts used = 66.67 mg/dm^3].

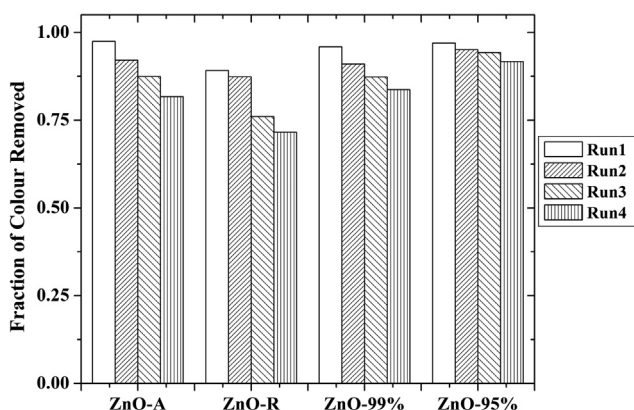


Figure 10 Stability and reusability of ZnO samples. [Volume of solution = 150 cm^3 ; catalysts used ZnO-R, ZnO-95%, ZnO-99% and ZnO-A; Initial dye concentration = 80 mg/dm^3 ; amount of catalysts used = 66.67 mg/dm^3 ; irradiation time = 150 min].

of $< 250\text{ nm}$. These particles exhibited comparable UV-catalytic activity with commercial nano-ZnO powders. The kinetics of photo-degradation reaction carried over MB dyes showed first order reaction kinetics for the ZnO samples having 1 mol% Y_2O_3 . When the Y_2O_3 doping exceeded 5 mol%, the catalytic reaction resulted in second order reaction kinetics. The segregation of Y_2O_3 appeared to be the reason. Highest photocatalyst efficiency was recorded at pH 10 for all the ZnO samples used in this study. Reusability studies confirmed that Yt doping improved the stability of the ZnO sample. With respect to reusability the samples could be ranked in the following order ZnO-95 > ZnO-99, ZnO-A > ZnO-R.

Acknowledgments

The third, fourth and fifth authors gratefully thank the SAS-TRA University Management for the financial support provided to this project through “Research and Modernization Fund” and are glad to acknowledge the help extended by the Associate Dean (Research), School of Chemical and Biotechnology, SAS-TRA University.

References

- Akyol, A., Yatmaz, H.C., Bayramoglu, M., 2004. Photocatalytic decolorization of Remazol Red RR in aqueous ZnO suspensions. *Appl. Catal. B* 54, 19–24.
- Al-Ekabi, Serpone, 1988. Kinetic studies in heterogeneous photocatalysis. I. Photocatalytic degradation of chlorinated phenols in aerated aqueous solutions over TiO₂ supported on a glass matrix. *J. Phys. Chem.* 92, 5726–5731.
- Amornpitoksuk, P., Suwanboon, S., Sangkanu, S., Sukhoom, A., Wudtipan, J., Srijan, K., Kaewtaro, S., 2011. Synthesis, photocatalytic and antibacterial activities of ZnO particles modified by diblock copolymer. *Powder Technol.* 212, 432–438.
- Ananthakumar, S., Anas, S., Ambily, J., Mangalaraja, R.V., 2010. Microwave assisted citrate gel combustion synthesis of ZnO Part-I, assessment of structural features. *J. Ceram. Process. Res.* 11, 29–34.
- Andelman, T., Gong, Y.Y., Polking, M., Yin, M., Kuskovsky, I., Neumark, G., O'Brien, S., 2005. Morphological control and photoluminescence of zinc oxide nanocrystals. *J. Phys. Chem. B* 109, 14314–14318.
- Atriabak, I., Bueno-Lopez, A., Garcia-Garcia, A., 2009. Role of yttrium loading in the physico-chemical properties and soot combustion activity of ceria and ceria-zirconia catalysts. *J. Mol. Catal. A: Chem.* 300, 103–110.
- Baran, W., Adamek, E., Makowski, A., 2008. The influence of selected parameters on the photocatalytic degradation of azo-dyes in the presence of TiO₂ aqueous suspension. *Chem. Eng. J.* 145, 242–248.
- Barka, N., Qourzal, S., Assabbane, A., Nounah, A., Ait-Ichou, Y., 2010. Photocatalytic degradation of an azo reactive dye, Reactive Yellow 84, in water using an industrial titanium dioxide coated media. *Arab. J. Chem.* 3, 279–283.
- Behnajady, M.A., Modirshahla, N., Hamzavi, R., 2006. Kinetic study on photocatalytic degradation of C.I. Acid Yellow 23 by ZnO photocatalyst. *J. Hazard. Mater. B* 133, 226–232.
- Beltran-Heredia, J., Torregrosa, J., Dominguez, J.R., Peres, J.A., 2001. Oxidation of *p*-hydroxybenzoic acid by UV radiation and by TiO₂/UV radiation: comparison and modelling of reaction kinetic. *J. Hazard. Mater. B* 83, 255–264.
- Daneshvar, N., Salari, D.G., Khataee, A.R., 2004. Photocatalytic degradation of azo dye acid red 14 in water on ZnO as an alternative catalyst to TiO₂. *J. Photochem. Photobiol. A* 162, 317–322.
- Fu, H., Xu, T., Zhu, S., Zhu, Y., 2008. Photocorrosion inhibition and enhancement of photocatalytic activity for ZnO via hybridization with C60. *Environ. Sci. Technol.* 42, 8064–8069.
- Gupta, V.K., Suhas, 2009. Application of low-cost adsorbents for dye removal – a review. *J. Environ. Manage.* 90, 2313–2342.
- Hammad, T.M., Salem, J.K., Harrison, R.G., 2009. Synthesis, characterization, and optical properties of Y³⁺-doped ZnO nanoparticles. *Nano* 4, 225–232.
- Hassan, K.H., 2010. Regeneration and activity test of spent zinc oxide hydrogen sulfide removal catalyst. *Eur. J. Sci. Res.* 39, 289–295.
- Hermann, J.M., 1999. Heterogeneous photocatalysis: fundamentals and applications. *Catal. Today* 5, 115–129.
- Jhung, S.H., Lee, J., Forster, P.M., Férey, G., Cheetham, K., Chang, J., 2006. Microwave synthesis of hybrid inorganic-organic porous materials, phase-selective and rapid crystallization. *Chem. Eur. J.* 12, 7899–7905.
- Jiang, Y., Sun, Y., Liu, H., Zhu, F., Yin, H., 2008. Solar photocatalytic decolorization of C.I. Basic Blue 41 in an aqueous suspension of TiO₂-ZnO. *Dyes Pigments* 78, 77–83.
- Kashefialasl, M., Khosravi, M., Marandi, R., Seyyedi, K., 2006. Treatment of dye solution containing colored index acid yellow 36 by electrocoagulation using iron electrodes. *Int. J. Environ. Sci. Technol.* 2, 365–371.
- Kim, S.H., Ngo, H.H., Shon, H.K., Vigneswaran, S., 2008. Adsorption and photocatalysis kinetics of herbicide onto titanium oxide and powdered activated carbon. *Sep. Purif. Technol.* 58, 335–342.
- Kohan, A.F., Ceder, G., Morgan, D., 2000. First-principles study of native point defects in ZnO. *Phys. Rev. B* 61, 19–27.
- Li, D., Haneda, H., 2003. Morphologies of zinc oxide particles and their effects on photocatalysis. *Chemosphere* 51, 129–137.
- Li, Y., Sun, S., Ma, M., Ouyang, Y., Yan, W., 2008. Kinetic study and model of the photocatalytic degradation of rhodamine B (RhB) by a TiO₂-coated activated carbon catalyst: Effects of initial RhB content, light intensity and TiO₂ content in the catalyst. *Chem. Eng. J.* 142, 147–155.
- Mangalampalli, V., Sharma, P., Durgakumari, V., Subrahmanyam, M., 2008. Solar photocatalytic degradation of isoproturon over TiO₂/H-MOR composite systems. *J. Hazard. Mater.* 160, 568–575.
- Moghaddam, A.B., Nazari, T., Badraghi, J., Kazemzad, M., 2009. Synthesis of ZnO nanoparticles and electrodeposition of polypyrrole/ZnO nanocomposite film. *Int. J. Electrochem. Sci.* 4, 247–257.
- Morrison, S.R., Freund, T., 1967. Chemical role of holes and electrons in ZnO photocatalysis. *J. Chem. Phys.* 47, 1543–1551.
- Perales-Perez, O.J., Tomar, M.S., Singh, S.P., Watanabe, A., Arai, T., Kasuya, A., Tohji, K., 2004. Ambient-temperature synthesis of nanocrystalline ZnO and its application in the generation of hydrogen. *Phys. Status Solidi* 1, 803–806.
- Ponnusami, V., Srivastava, S.N., 2009. Studies on application of teak leaf powders for the removal of color from synthetic and industrial effluents. *J. Hazard. Mater.* 169, 1159–1162.
- Ravinder, K., Singh, A.V., Kiran, S., Mehra, N.C., Mehra, R.M., 2006. Sol-gel derived yttrium doped ZnO nanostructures. *J. Non-Cryst. Solids* 352, 396.
- Sancier, K.M., Morrison, S.R., 1973. Oxidation of organic molecules by photoproduced holes of ZnO. *Surf. Sci.* 36, 622–629.
- Sun, S.H., Zeng, H., Robinson, Raoux, D.B., Rice, P.M., Wang, S.X., 2004. Monodisperse MFe₂O₄ (M = Fe, Co, Mn) nanoparticles. *J. Am. Chem. Soc.* 126, 273–279.
- Velmurugan, R., Selvam, K., Krishnakumar, B., Swaminathan, M., 2011. An efficient reusable and antiphotocorrosive nano ZnO for the mineralization of reactive orange 4 under UV-A light. *Sep. Purif. Technol.* 80, 119–124.
- Wu, C.H., Chang, H.W., Chern, J.M., 2006. Basic dye decomposition kinetics in a photocatalytic slurry reactor. *J. Hazard. Mater. B* 137, 336–343.
- Wu, J.-S., Liu, C.-H., Chu, K.H., Suen, S.-Y., 2008a. Removal of cationic dye methyl violet 2B from water by cation exchange membranes. *J. Membrane Sci.* 309, 239–245.
- Wu, Z., Wang, H., Liu, Y., Jiang, B., Sheng, Z., 2008b. Study of a photocatalytic oxidation and wet absorption combined process for removal of nitrogen oxides. *Chem. Eng. J.* 144, 221–226.